

Fast Graphlet Transform of Sparse Graphs

Dimitris Floros*

Nikos Pitsianis*†

Xiaobai Sun†

*Department of Electrical and Computer Engineering
Aristotle University of Thessaloniki
Thessaloniki 54124, Greece

†Department of Computer Science
Duke University
Durham, NC 27708, USA

Abstract—We introduce the computational problem of graphlet transform of a sparse large graph. Graphlets are fundamental topology elements of all graphs/networks. They can be used as coding elements to encode graph-topological information at multiple granularity levels for classifying vertices on the same graph/network as well as for making differentiation or connection across different networks. Network/graph analysis using graphlets has growing applications. We recognize the universality and increased encoding capacity in using multiple graphlets, we address the arising computational complexity issues, and we present a fast method for exact graphlet transform. The fast graphlet transform establishes a few remarkable records at once in high computational efficiency, low memory consumption, and ready translation to high-performance program and implementation. It is intended to enable and advance network/graph analysis with graphlets, and to introduce the relatively new analysis apparatus to graph theory, high-performance graph computation, and broader applications.

Index Terms—network analysis, topological encoding, fast graphlet transform

I. INTRODUCTION

Network analysis using graphlets has advanced in recent years. The concepts of graphlets, graphlet frequency, and graphlet analysis are originally introduced in 2004 by Pržulj, Corneil and Jurisica [12]. They are substantially extended in a number of ways [8], [16], [19], [21]. Graphlets are mostly used for statistical characterization and modeling of entire networks. In the work by Palla et. al. [10], which is followed by many, a network of motifs (a special case of graphlets) is induced for overlapping community detection on the original network. Recently we established a new way of using graphlets for graph analysis. We use graphlets as coding elements to encode topological and statistical information of a graph at multiple granularity levels within a graph, from micro-scale structures at vertex neighborhoods, up to macro-scale structures such as cluster configurations [5]. We also use the topology encoded information to uncover temporal patterns of variation and persistence across networks in a time-shifted sequence, not necessarily over the same vertex set [6].

We anticipate a growing interest in, and applications of, graphlet-based network/graph analysis, for the following reasons. Graphlets are fundamental topology elements of all networks or graphs. See a particular graphlet dictionary shown in Fig. 1. Conceptually, graphlets for network/graph analysis are similar to wavelets for spectro-temporal analysis in signal processing [15], shapelets for time series classification [22], super-pixels for image analysis [14], and n-grams for natural

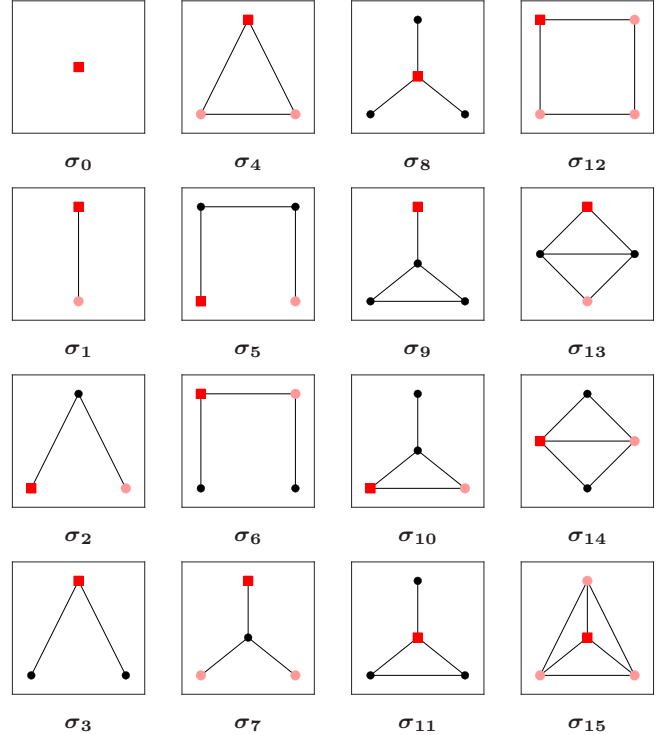


Fig. 1: Dictionary Σ_{16} of 16 graphlets. In each graphlet, the designated incidence node is specified by the red square marker, its automorphic position(s) specified by red circles. The total ordering (labeling) of the graphlets is by the following nesting conditions. The graphlets are ordered first by non-decreasing number of vertices. Graphlets with the same vertex set belong to the same family. Within each family, the ordering is by non-decreasing number of edges, and then by increasing degree at the incidence node (except the 4-cycle). The inclusion of σ_0 is necessary to certain vertex partition analysis [5].

language processing [17], [18]. Like motifs, graphlets are small graphs. By conventional definition, motifs are small subgraph patterns that appear prescriptively and significantly more frequently in a network under study. Motif analysis relies on prior knowledge or assumption [7]. Graphlets are ubiquitous; graphlet analysis reveals the most frequent connection patterns or motifs, or lack of dominance by any, in a network.

There is another aspect of the universality in using graphlets. Graphlets are defined in the graph-topology space. They are not to be confused with the wavelets applied to the spectral elements of a particular graph Laplacian as in certain algebraic graph analysis. The latter is limited to the family of graphs defined on the same vertex set and share the same eigenvectors.

Otherwise, the Laplacians of two graphs even defined on the same vertex set are not commutable. The computation of Laplacian spectral vectors and values is also limited, by computational complexity and resource, to low dimensional invariance subspaces.

The time and space complexities of graph encoding with graphlets, i.e., the graphlet transform, have not been formally described and addressed. We describe the graphlet transform in Section II, with which we obtain the graphlet frequencies at all vertices on a network/graph. In fact, this is related to the classical problem of finding, classifying and counting small subgraphs over vertex neighborhoods [4], [13]. A familiar case is to find and count all triangles over the entire graph. The triangle is graphlet σ_4 (C_3, K_3) in the dictionary in Fig. 1. With the graphlet transform, we count in more detail – the number of distinct triangles incident on each and every vertex. We found from our recent analysis of scientific collaboration networks [6] that the bi-fork graphlet σ_3 ($K_{1,2}$) encodes the betweenness between triangle clusters. The bi-fork betweenness is to be calculated at each and every vertex. Another familiar case is to find and count induced subgraphs with the pattern of the claw graphlet σ_8 ($K_{1,3}$). The time complexity for calculating the number of claws over all vertices of graph $G = (V, E)$ is $O(n^4)$, $n = |V|$, by the naive method that checks every connected quad-node subgraph to see if it is a claw. The naive method can be accelerated in asymptotic complexity by applying fast matrix multiplication algorithms on asymptotically sufficiently large graphs, at the expense of greater algorithmic complication, and if feasible to implement, with increased memory consumption, loss of data locality and increased latency in memory access on any modern computer with hierarchical memory. Due to the high complexity, some network analysis with graphlets resort to nondeterministic approximation with sparse sampling under a necessary structure-persistent assumption [13]. It is known otherwise that certain network properties are not preserved with sampling [20].

The present work makes a few key contributions. We formally introduce the graphlet transform problem, and address both the encoding capacity and the encoding complexity issues. We present the fast method for graphlet transform of any large, sparse graph, with any sub-dictionary of Σ_{16} as the coding basis. The solution is deterministic, exact and directly applicable to any range of graph size. Our solution method establishes remarkable records at once in multiple aspects – time complexity, memory space complexity, program complexity and high-performance implementation. Particularly, the time complexity of the fast graphlet transform with any dictionary $\Sigma \subseteq \Sigma_{16}$ is linear in $(|V| + |E|)|\Sigma|$ on degree-bounded graphs. The transform formulas can be straightforwardly translated to high performance computation, via the use of readily available software libraries such as GraphBLAS¹. We also address on criteria of selecting graphlet elements for certain counting-based decision or detection problems on graphs. Our objectives

of developing the fast graphlet transform are twofold: to enable large network/graph analysis with graphlets and to enrich and advance sparse graph theory, computation and their applications.

We describe the basic assumptions and notations in the rest of the paper. Graph $G = (V, E)$ has $n = |V|$ nodes/vertices and $m = |E|$ edges/links. It is sparse, i.e., m is of the order $n \log^k n$ with a small value of k . The nodes are indexed from 1 to n , a particular ordering is specified when necessary. Graph G is undirected and specified by its (symmetric) adjacency matrix A of 0-1 values. The j -th column of A , denoted by a_j , marks the neighbors of node j . Denote by e_j the j -th column of the identity matrix. The sum of all e_j is the constant-1 vector, denoted by e . The maximal degree is d_{\max} . The Hadamard (elementwise) multiplication is denoted by \odot . The number of nonzero elements in matrix B is $\text{nnz}(B)$. The total number of arithmetic operations for constructing B is $\text{cost}(B)$. Let a and b be non-negative vectors. We use $a - b$ as the shorthand expression for the sparse difference, i.e., the rectified difference $\max\{a - b, 0\}$. The notations are rarely repeated for brevity.

II. GRAPHLET TRANSFORM: PROBLEM DESCRIPTION

We now describe generic graphlets and graphlet dictionaries by their forms and attributes, with modification in description over the original for clarity. A *graphlet* is a connected graph with a small vertex set and a unique orbit (a subset of vertices symmetric under permutations). We show in Fig. 1 a dictionary of 16 graphlets, $\Sigma = \Sigma_{16} = \{\sigma_k\}_{k=0:15}$. The graphlets in the dictionary have the following patterns: singleton/vertex, edge (K_2), 2-path (P_2), binary fork ($K_{1,2}$), triangle (C_3, K_3), 3-path (P_3), claw ($K_{1,3}$), dippers, 4-cycle (C_4), diamonds, and tetrahedral (K_4). Each graphlet has a designated incidence node, shown with a red square, unique up to an isomorphic permutation (shown in red circles). In short, Σ_{16} contains all connected graphs up to 4 nodes with distinctive vertex orbits. Graphlets on the same vertex set form a family with an internal partial ordering. For example, in the tri-node family, the partial ordering $\sigma_2, \sigma_3 \prec \sigma_4$ denotes the relationship that σ_2 and σ_3 are subgraphs of σ_4 . Our rules for the ordering/labeling are described in the caption of Fig. 1 for convenience in visual verification.

Let $G = (V, E)$ be a graph. Let Σ be a graphlet dictionary, the code book. We use a vertex-graphlet incidence structure to describe the process of encoding G over the entire vertex set V with coding elements in Σ . Denote by $B = (V, \Sigma; E_{v\sigma})$ the bipartite between the graph vertices and the graphlets, $E_{v\sigma} \subseteq V \times \Sigma$. There is a link (v, σ) between a vertex $v \in V$ and a graphlet $\sigma \in \Sigma$ if v is an incident node on a subgraph of σ -pattern. The incident node on a graphlet is uniquely specified, up to an isomorphic mapping. For example, graphlet σ_6 (clique K_4) in Fig. 1 is an automorphism. There may be multiple links between v and σ_k . We denote them by a single link (v, σ_k) with a positive integer weight $d_k(v)$ for the multiplicity, which is the frequency with graphlet σ_k . However, the multiplicities from vertex v to multiple graphlets in the same family are

¹<http://graphblas.org>

not independently determined. For example, the multiplicities on links from vertices to σ_2 do not include those within σ_4 . The weight on (v, σ_1) is counted independently as σ_1 has no other family member. For any vertex, $d_0(v) = 1$, $d_1(v)$ is the ordinary degree of v on graph G . With $k > 1$, $d_k(v)$ is a pseudo degree, depending on the internal structure of the family σ_k is in. This vertex-graphlet incidence structure is a generalization of the ordinary vertex-edge incidence structure.

The *graphlet transform* of graph G refers to the mapping f of G to the field of graphlet frequency vectors over V ,

$$f(v) = [d_0(v), d_1(v), \dots, d_{|\Sigma|-1}(v)]^T, \quad v \in V. \quad (1)$$

The vector field encodes the topological and statistical information of the graph. The transform is orbit-invariant, i.e., for u and v on the same orbit, $f(u) = f(v)$. It is graph invariant, i.e., for isomorphic graphs G and G' , $G \simeq G'$, $f(G) = f(G')$. In this paper we introduce how we make the transform fast.

Consider first the coding capacity. The dictionary $\Sigma_2 = \{\sigma_0, \sigma_1\}$ is the minimal. It limits the network analysis to the ordinary degree distributions, types, correlations and models [1], [9], [11]. The dictionary Σ_5 , a sub-dictionary of Σ_{16} , already offers much greater coding capacity. We address and answer an additional, interesting question – how the computation complexity changes with the choice of the coding elements.

III. FAST GRAPHLET TRANSFORM WITH Σ_5

A. Preliminary: graph of paths & graph of cycles

We start with graphs of paths and graphs of cycles, using matrix expressions and operations. Denote by $G(P_\ell)$ the graph of length- ℓ paths over G with weighted adjacency matrix P_ℓ , $\ell > 0$. Element $P_\ell(i, j)$ is the number of length- ℓ , simple (i.e., loop-less) paths between node i and node j . Let $p_\ell = P_\ell e$. It represents the scalar function on V such that $p_\ell(i)$ is the total number of length- ℓ paths with node i at one of the ends. In particular, $P_1 = A$, $p_1 = d_1$. We have

$$P_2 = A^2 - \text{diag}(d_1), \quad (2)$$

where ‘diag’ denotes the construction or extraction of a diagonal matrix. We describe the important fact that every edge $(i, j) \in E$ makes connection between node j (node i) to the neighbors of node i (node j), not including itself.

Lemma 1 (Matrix of 2-paths.). *Matrix P_2 is the accumulation of 2-column contribution from each and every edge,*

$$P_2 = \sum_{(i,j) \in E} (a_i - e_j)e_j^T + (a_j - e_i)e_i^T. \quad (3)$$

Consequently,

$$\text{nnz}(P_2) \leq \text{cost}(P_2) < 2 \cdot d_{\max} \cdot m. \quad (4)$$

Similarly, $A^2 = \sum_{(i,j)} a_i e_j^T + a_j e_i^T$. Lemma 1 plays a fundamental role in subsequent complexity analysis.²

²The simple expressions for A^2 and P_2 were not seen in graph analysis literature.

Denote by $G(C_\ell)$ the graph of length- ℓ cycles over G with weighted adjacency matrix C_ℓ , $\ell > 1$. Element $C_\ell(i, j)$ is the number of length- ℓ simple cycles that pass through both i and j . We denote by c_ℓ the vertex function on V such that $c_\ell(i)$ is the total number of length- ℓ simple cycles passing through node i . A simple cycle is a simple path that starts from and ends at the same node. We state an important property of the graph of ℓ -cycles.

Lemma 2 (Sparse graph of cycles). *For $\ell > 1$, matrix C_ℓ is as sparse as A ,*

$$C_\ell = A \odot P_{\ell-1}, \quad (5)$$

In addition, $c_\ell = C_\ell e / (\ell - 1)$. Particularly, $c_2 = d_1$, $C_3 = A \odot A^2$ and $c_3 = C_3 e / 2$.

An immediate consequence of the lemma is the alternative formulation of p_2 ,

$$p_2 = A p_1 - c_2, \quad (6)$$

without forming matrix P_2 .

B. Tri-node graphlet frequencies

There are 3 members in the tri-node graphlet family. Graphlet σ_2 is the 2-path, with the incidence node at an end. Graphlet σ_3 is the bi-fork, $K_{1,2}$, with the incidence node at the root. Graphlet σ_4 is the triangle, i.e., 3-cycle C_3 or 3-clique K_3 . There is a partial ordering within the family,

$$\sigma_2, \sigma_3 \prec \sigma_4, \quad (7)$$

by the relationship that σ_4 , the triangle, has σ_2 and σ_3 as subgraphs. The frequency with σ_2 at node i in graph G does not include those σ_2 subgraphs in any triangle. Similarly with the σ_3 frequency at any node.

Lemma 3 (Bi-fork graphlet frequencies). *The bi-graphlet frequency vector can be expressed as follows,*

$$d_3 = p_1 \odot (p_1 - 1)/2 - 2 c_3. \quad (8)$$

Recall that we already have the vertex functions/vectors $d_0 = e$, $d_1 = A e$ and $d_4 = c_3$. It is straightforward to verify that $d_2 = p_2 - c_3$. Together, we have the following theorem.

Theorem 1 (Fast graphlet transform with Σ_5). *The graphlet transform of $G = (V, E)$ with Σ_5 takes $\alpha \cdot d_{\max} \cdot m$ arithmetic operations and $\beta \cdot (m + n)$ memory space, $\alpha < 3$ and $\beta < 6$.*

IV. FAST GRAPHLET TRANSFORM WITH Σ_{16}

We turn our attention to the family of quad-node graphlets. The family has 11 members (σ_5 to σ_{15}) with the following partial ordering in terms of subgraph relationship,

$$\begin{aligned} & \sigma_5, \sigma_6 \prec \sigma_9, \sigma_{10}, \sigma_{11}, \sigma_{12}; \\ & \sigma_7, \sigma_8 \prec \sigma_9, \sigma_{10}, \sigma_{11}; \\ & \sigma_9, \sigma_{10}, \sigma_{11}, \sigma_{12} \prec \sigma_{13}, \sigma_{14}; \\ & \sigma_{13}, \sigma_{14} \prec \sigma_{15}. \end{aligned} \quad (9)$$

With each graphlet σ_i we derive first the formula for its raw or independent frequency at vertex v , denoted by

$\hat{d}_i(v)$, as the number of σ -pattern subgraphs incident with v . The subgraphs include the induced ones. The raw frequency vector is $\hat{f}(v) = [\hat{d}_0(v), \hat{d}_1(v), \dots, \hat{d}_{|\Sigma|-1}(v)]^T$. We will then convert the raw frequencies to the nested, or *net*, frequencies of (1). The net frequencies depend on the inter-relationships between the graphlets in a dictionary, as shown by the partial ordering in (9) for Σ_{16} . We always have $\hat{f}(v) \geq f(v)$. We shall clarify the connection between net frequencies and induced subgraphs. When, and only when, the family of k -node graphlets is complete with distinctive connectivity patterns and orbits and non-redundant, the net frequency of graphlet σ at vertex v is the number of σ -pattern *induced* subgraphs incident with v . For instance, a 3-star (claw) subgraph in a dipper is not the induced graph by the same vertex set. Under the complete and non-redundant family condition, the frequency conversion has the additional functionality to identify precisely the patterns of induced subgraphs. We will describe in Section V a unified scheme for converting raw frequencies to net ones. The condition on graphlet families can be relaxed for graph encoding purposes other than pattern recognition. We derive fast frequency formulas for quad-node graphlets in 3 subgroups.

A. The 3-paths & 4-cycle

We relate the frequencies with 3-path graphlet σ_5 and gate graphlet σ_6 to that with p_1 and p_2 . The following are straightforward.

$$\hat{d}_5 = p_3, \quad \hat{d}_6 = p_2 \odot (p_1 - 1) - 2c_3. \quad (10)$$

Lemma 4 (Fast calculation of 3-path frequencies).

$$p_3 = A p_2 - p_1 \odot (p_1 - 1) - 2c_3. \quad (11)$$

Proof. We get $p_3 = P_3 e$ by the expression of

$$P_3 = A P_2 - \text{diag}(p_1 - 1) P_1 - 2 \text{diag}(c_3), \quad (12)$$

where we extend P_2 by one step walk, remove 1-step backtrack, and remove triangles on the diagonal. \square

By the lemma, vector p_3 is obtained without formation of P_3 , which invokes the cubic power of A . Next, we obtain vector c_4 without constructing $C_4 = A \odot P_3$ of Lemma 2.

Lemma 5 (Fast calculation of 4-cycle frequencies). Denote by $G(C_{4,2})$ the graph with adjacency matrix $C_{4,2}$ such that element $C_{4,2}(i, j)$ is the number of distinct 4-cycles passing through two nodes i and j at diametrical positions. Then,

$$C_{4,2} = P_2 \odot (P_2 - 1), \quad c_4 = C_{4,2} e/2. \quad (13)$$

Consequently, $\text{nnz}(C_{4,2}) \leq \text{nnz}(P_2)$.

By the diametrical symmetry, $\sum_j C_{4,2}(i, j)$ is twice the total number of 4-cycles passing through i . Matrix $C_{4,2}$ may be much sparser than P_2 of Lemma 1.

The essence of our fast frequency calculation lies in constructing sparse auxiliary matrices and vectors which use Hadamard products for both logical conditions and multiplicative aggregations, instead of limiting to either only logical

operations (such as in circuit expressions) or only arithmetic operations (such as in counting methods that resort to fast matrix-matrix products). By the same principal approach, we present the formulas for fast calculation of the remaining 8 graphlet frequencies with very brief statements and proof sketches, within the text space limit.

B. The claws & dippers

This section contains fast formulas for raw frequencies with two claw graphlets and three dipper graphlets. Graphlet σ_7 is the claw with the incidence node at a leaf node. At node i , we sum up the bi-fork counts over its p_1 neighbors, excluding the one connecting to i , i.e., $(p_1(i) - 1)$ choose 2. Thus,

$$\hat{d}_7 = A \cdot ((p_1 - 1) \odot (p_1 - 2))/2. \quad (14)$$

Graphlet σ_8 is the claw ($K_{1,3}$) with the incidence node at the root/center. We have

$$\hat{d}_8 = p_1 \odot (p_1 - 1) \odot (p_1 - 2)/3!, \quad (15)$$

by the fact that the number of 3-stars centered at a node i is $p_1(i)$ choose 3.

Graphlet σ_9 is the dipper with the incidence node at the handle end. We have

$$\hat{d}_9 = A c_3 - 2 c_3. \quad (16)$$

The triangles passing i are removed from the total number of triangles incident at the neighbor nodes of i .

Graphlet σ_{10} is the dipper with the incidence node at a base node. We have

$$\hat{d}_{10} = C_3 (p_1 - 2). \quad (17)$$

Each triangle at node i is multiplied by the number of other adjacent nodes that are not on the same triangle. By Lemma 2, C_3 is as sparse as A .

Graphlet σ_{11} is the dipper with the incidence node at the center (degree 3). We have

$$\hat{d}_{11} = (p_1 - 2) \odot c_3. \quad (18)$$

At the incident node i , the number of triangles is multiplied by all other edges leaving node i .

For this group of graphlets, the calculation of the raw frequencies uses either vector operations or matrix-vector products with the matrix as A itself or as sparse as A .

C. The diamonds & the tetrahedral

Graphlet σ_{13} is the diamond with the incidence node at an off-cord node i . We have

$$D_4 \triangleq A \odot (A(C_3 - A)), \quad \hat{d}_{13} = D_4 e/2. \quad (19)$$

Proof. In a diamond with i as an off-cord node, two neighbor nodes in a_i must be on the cord connecting the triangle with i and another triangle. Thus, the account for i on each of the off-cord nodes is $a_i^T (C_3 - 1) a_i = a_i^T (C_3 - A) a_i$, or equally, $(a_i^T \odot (a_i^T (C_3 - A))) e$. \square

By Lemma 2, matrix $(C_3 - A)$ is no denser than A , $\text{cost}(D_4) < \text{cost}(P_2)$, see Lemma 1.

Graphlet σ_{14} is the diamond with the incidence node at a cord node. We have

$$\hat{d}_{14} = (A \odot C_{4,2}) e/2. \quad (20)$$

The Hadamard product is sparse, $C_{4,2}$ is defined in Lemma 5.

Proof. Node i on a 4-cycle must be connected with its diametrical node. \square

Graphlet σ_{15} is clique K_4 . Define matrix T as follows,

$$T \triangleq A \odot [q_{ij}^T A q_{ij}], \quad q_{ij} = a_i \odot a_j, \quad (21)$$

where a_j is the column j of A . We have

$$\hat{d}_{15}(i) = T e/6. \quad (22)$$

Proof. For $(i, j) \in E$, q_{ij} indicates the common neighbors between node i and node j . When $q_{ij}(k)q_{ij}(\ell)A(k, \ell) \neq 0$, the subgraph at $\{i, j, k, \ell\}$ is a tetrahedral. The total number of distinct tetrahedrals incident with edge (i, j) is $T(i, j) = \sum_{k > \ell} q_{ij}(k)q_{ij}(\ell)A(k, \ell)/3 = q_{ij}^T A q_{ij}/6$. \square

Matrix T is sparse. For $(i, j) \in E$, computing $T(i, j)$ takes no more than $3 \text{nnz}(q_{ij})^2$ arithmetic operations.

V. A UNIFIED SCHEME FOR FREQUENCY CONVERSION

We summarize in Table 1 the formulas in matrix-vector form for fast calculation of the raw frequencies. The auxiliary vectors are p_j and c_j , $1 \leq j \leq 4$, each of which is elaborated in sections III and IV. The auxiliary matrices C_3 , $A \odot C_{4,2}$, D_4 and T are as sparse as A .

We provide in Table 2 the (triangular) matrix U_{16} of nonnegative coefficients for mapping net frequencies $d(v)$ to raw frequencies $\hat{d}(v)$. The conversion coefficients are determined by subgraph-isomorphisms among graphlets and automorphisms in each graphlet. The frequency conversion for any sub-dictionary of Σ_{16} is by the corresponding submatrix of U_{16} . We actually use the inverse mapping to filter out non-induced subgraphs. The conversion matrix, invariant across the vertices, is applied to each and every vertex. The conversion complexity is proportional to the product of $|V|$ and the number of nonzero elements in the conversion matrix. The number of nonzero elements in U_{16} is less than $3|\Sigma_{16}|$. The inverse U_{16}^{-1} has exactly the same sparsity pattern as U_{16} . The identical sparsity property also holds between each sub-dictionary conversion matrix and its inverse.

We illustrate in Fig. 2 the graphlet transform of a small graph $G = (V, E)$ with 6 vertices and 9 edges. With each graphlet σ_i , the raw frequencies \hat{d}_i across all vertices are calculated by the fast formulas in Table 1 and tabulated in the top table/counts computed by our fast transforms. The i -th row in the table is the raw frequency vector $\hat{f}^T(v_i)$. The raw frequency vectors are converted to the net frequency vectors $\{f(v), v \in V\}$ of (1) by matrix-vector multiplications with the same triangular matrix U_{16}^{-1} . As the fast graphlet transform is exact, we made accuracy comparison between the results by our sparse and fast formulas and that by the dense counterparts. The results are in full agreement. The

TABLE 1: Formulas for fast calculation of raw graphlet frequencies on the vertices of a graph G with adjacency matrix A , with respect to graphlet dictionary Σ_{16} as shown in Fig. 1. The auxiliary vectors and matrices are specified in Sections III and IV. The rectified difference $\max\{b-a, 0\}$ between two vectors a and b is denoted simply as $b-a$.

Σ_{16}	Graphlet, incidence node	Formula in vector expression
σ_0	singleton	$\hat{d}_0 = e$
σ_1	1-path, at an end	$\hat{d}_1 = p_1$
σ_2	2-path, at an end	$\hat{d}_2 = p_2$
σ_3	bi-fork, at the root	$\hat{d}_3 = p_1 \odot (p_1 - 1)/2$
σ_4	3-clique, at any node	$\hat{d}_4 = c_3$
σ_5	3-path, at an end	$\hat{d}_5 = p_3$
σ_6	3-path, at an interior node	$\hat{d}_6 = p_2 \odot (p_1 - 1) - 2c_3$
σ_7	claw, at a leaf	$\hat{d}_7 = A \cdot ((p_1 - 1) \odot (p_1 - 2))/2$
σ_8	claw, at the root	$\hat{d}_8 = p_1 \odot (p_1 - 1) \odot (p_1 - 2)/6$
σ_9	dipper, at the handle tip	$\hat{d}_9 = A \cdot c_3 - 2c_3$
σ_{10}	dipper, at a base node	$\hat{d}_{10} = C_3 \cdot (p_1 - 2)$
σ_{11}	dipper, at the center	$\hat{d}_{11} = (p_1 - 2) \odot c_3$
σ_{12}	4-cycle, at any node	$\hat{d}_{12} = c_4$
σ_{13}	diamond, at an off-cord node	$\hat{d}_{13} = D_4 \cdot e/2$
σ_{14}	diamond, at an on-cord node	$\hat{d}_{14} = (A \odot C_{4,2}) \cdot e/2$
σ_{15}	4-clique, at any node	$\hat{d}_{15} = T \cdot e/6$

transform has additional values in systematic quantification and recognition of topological properties of the graph, as briefly noted in the caption of Fig. 2.

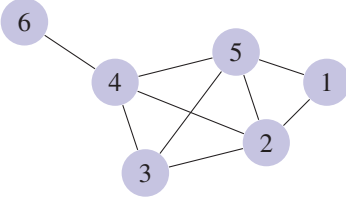
TABLE 2: The matrix U_{16} for conversion from net frequencies to raw frequencies, $U_{16}f = \hat{f}$, associated with dictionary Σ_{16} . The raw-to-net frequency conversion $f = U_{16}^{-1}\hat{f}$ is used in the fast transform. All coefficients of U_{16} are non-negative. A sub-dictionary with index set s has the conversion matrix $U_{16}(s, s)$, $\{0, 1\} \subseteq s \subseteq \{0, 1, \dots, 15\}$.

U_{16}	d_0	d_1	d_2	d_3	d_4	d_5	d_6	d_7	d_8	d_9	d_{10}	d_{11}	d_{12}	d_{13}	d_{14}	d_{15}
d_0	1															
d_1		1														
d_2			1	2												
d_3				1	1											
d_4					1											
d_5						1			2	1		2	4	2	6	
d_6							1			1	2	2	2	4	6	
d_7								1	1	1			2	1	3	
d_8									1			1		1	1	
d_9										1			2		3	
d_{10}											1		2	2	6	
d_{11}												1		2	3	
d_{12}												1	1	1	3	
d_{13}													1		3	
d_{14}														1		
d_{15}																1

VI. HIGH-PERFORMANCE GRAPHLET TRANSFORM

We address the high-performance aspect of graphlet transform. The fast graphlet has the distinguished utility property that the formulas are simple and in ready form to be translated to high-performance program and implementation. We highlight three conceptual and operational issues key to high-performance implementation.

The first is on the use of sparse masks. We exploit graph sparsity in every fast formula. This is to be formally translated into any implementation specification: every sparse operation



v	\hat{d}_0	\hat{d}_1	\hat{d}_2	\hat{d}_3	\hat{d}_4	\hat{d}_5	\hat{d}_6	\hat{d}_7	\hat{d}_8	\hat{d}_9	\hat{d}_{10}	\hat{d}_{11}	\hat{d}_{12}	\hat{d}_{13}	\hat{d}_{14}	\hat{d}_{15}
1	1	2	6	1	1	14	4	6	0	6	4	0	2	2	0	0
2	1	4	9	6	4	12	19	7	4	3	12	8	5	3	5	1
3	1	3	9	3	3	14	12	9	1	5	12	3	4	4	3	1
4	1	4	8	6	3	12	18	7	4	5	10	6	4	4	3	1
5	1	4	9	6	4	12	19	7	4	3	12	8	5	3	5	1
6	1	1	3	0	0	8	0	3	0	3	0	0	0	0	0	0

v	d_0	d_1	d_2	d_3	d_4	d_5	d_6	d_7	d_8	d_9	d_{10}	d_{11}	d_{12}	d_{13}	d_{14}	d_{15}
1	1	2	4	0	1	2	0	0	0	2	0	0	0	2	0	0
2	1	4	1	2	4	0	1	0	0	0	2	1	0	0	2	1
3	1	3	3	0	3	0	0	0	0	0	4	0	0	1	0	1
4	1	4	2	3	3	0	2	0	0	0	2	3	0	1	0	1
5	1	4	1	2	4	0	1	0	0	0	2	1	0	0	2	1
6	1	1	3	0	0	2	0	0	0	3	0	0	0	0	0	0

Fig. 2: An illustration of graphlet transform: the graph $G = (V, E)$ to the left, with $|V| = 6$ and $|E| = 9$, is transformed to the net frequency vector field $\{f(v), v \in V\}$ placed in the bottom table to the right, with respect to dictionary Σ_{16} . The net frequencies are converted from the raw frequencies vector field $\{f(v), v \in V\}$ in the top table. **Observations.** The transform quantifies and recognizes topological properties of graph G . The vertices in the same orbit have the same frequency vectors, $f(v_2) = f(v_5)$; G has 5 triangles, $\text{sum}(d_4)/3 = 5$; G is free of 4-cycles, $d_{12} = 0$; and free of claws, $d_7 = d_8 = 0$.

is associated with source mask(s) on input data and target mask on output data. Particularly, an unweighted adjacency matrix serves as its own sparsity mask. Masked operations are supported by GraphBLAS, the output matrix/vector is computed or modified only where the mask elements are on, not off. A simple example is the Hadamard product of two matrices. As the intersection of two source masks, the target mask is no denser than any of the source masks. Often, a factor matrix is either the adjacency matrix A itself or as sparse as A . A non-trivial example is the chain of masks with a sequence of sparse operations. For example, in calculating the scalar $v^T A v$ with sparse vector v and sparse matrix A , as in (19) or (21), the target mask for Av is the nonzero pattern of v . With sparse masks, we reduce or eliminate unnecessary operations, memory allocation and memory accesses.

The next two issues are closely coupled: operation scheduling and performing computations on-the-fly. The objective is two-fold: (i) to minimize the number of revisits to the same matrix or vector elements, and (ii) to reduce the amount of working space memory. Operations using the same auxiliary matrix are carried out together with updates on the output while auxiliary matrix elements are computed on the fly. No auxiliary matrix is explicitly stored. With our first implementation, the space complexity is $2m + n(|\Sigma| + 2)$. We acknowledge additional benefits with GraphBLAS in sparse storage format and parallel implementation on modern multi-core computers [2], [3].

VII. MAIN THEOREM & BEYOND

By the preceding analysis we have the following theorem.

Theorem 2 (Fast graphlet transform with Σ_{16}). *Let Σ be a graphlet dictionary, $\Sigma \subseteq \Sigma_{16}$. Let $G = (V, E)$ be a sparse graph. The fast graphlet transform of G , by the formulas in Table 1 and the frequency conversion in Table 2, has the time and space complexities bounded from above as follows.*

(a) *Upper bounds on time complexity:*

$$(\alpha d_{\max} m + 3n) |\Sigma|, \quad \alpha < 10, \quad \sigma_{15} \notin \Sigma,$$

$$(\beta (c d_{\max} + d^2(n_c))m + 3n) |\Sigma|, \quad \beta < 5, \quad \sigma_{15} \in \Sigma,$$

where c is a constant, $c < d_{\max}$, $d(j)$ is the degree of node j in non-increasing order, $n_c = \lfloor c m / d_{\max} \rfloor < n$.³

(b) *Upper bound on space complexity:* $2m + n(|\Sigma| + 2)$.

We remark on dictionary capacity and selection criteria. A larger dictionary offers an exponentially increased encoding range at only linearly increased computation cost. Depending on the object of graphlet encoding, certain graphlets must be included together. For example, when we use the bi-fork σ_3 to encode the betweenness among triangle clusters, the triangle graphlet σ_4 must be included [6]. For another example, for claw-free recognition, it is necessary to include σ_{11} , σ_{14} and σ_{15} which have 3-stars as subgraphs.

To our knowledge, the fast graphlet transform establishes a few remarkable records. It enables the use of graphlets for analysis of large sparse networks. When applied to certain counting-based decision problems, the complexities are of the same order as, or even lower than, the best existing asymptotic complexities that resort to unreachable, materializable size. The time complexity on degree-bounded graphs is linear with $(m + n)$. This includes triangle, diamond or claw detection, and if detected, with precise vertex locations. When d_{\max} varies with n and G is sparse, $d^2(n_c)$ is likely smaller than d_{\max} with many large real-world or model generated networks. The complexity analysis for d_{15} involves partition of V and a partition of the edge-vectors q_{ij} , $(i, j) \in E$, by sparsity patterns, for computing matrix T of (21). We omit the details.

Our transform method with fast formulas for raw frequencies with graphlets and fast frequency conversion can be tailored for faster analysis of certain graph-topology recognition problems, which are beyond the scope of this paper.

³Architecture-dependent memory operations are not included.

REFERENCES

- [1] A.-L. Barabási and M. Pósfai, *Network Science*. Cambridge, UK: Cambridge University Press, 2016.
- [2] A. Buluç, J. T. Fineman, M. Frigo, J. R. Gilbert, and C. E. Leiserson, “Parallel sparse matrix-vector and matrix-transpose-vector multiplication using compressed sparse blocks,” in *Proceedings of the 21st Annual Symposium on Parallelism in Algorithms and Architectures*, 2009, pp. 233–244.
- [3] T. A. Davis, “Graph algorithms via SuiteSparse: GraphBLAS: Triangle counting and K-truss,” in *2018 IEEE High Performance Extreme Computing Conference (HPEC)*, 2018, pp. 1–6.
- [4] R. A. Duke, H. Lefmann, and V. Rödl, “A fast approximation algorithm for computing the frequencies of subgraphs in a given graph,” *SIAM Journal on Computing*, vol. 24, no. 3, pp. 598–620, 1995.
- [5] D. Floros, T. Liu, N. P. Pitsianis, and X. Sun, “Measures of Discrepancy between Network Cluster Configurations using Graphlet Spectrograms,” 2020, manuscript under review.
- [6] ———, “Using graphlet spectrograms for temporal pattern analysis of virus-research collaboration networks,” in *2020 IEEE High Performance Extreme Computing Conference (HPEC)*, 2020, to appear.
- [7] R. Milo, “Network motifs: Simple building blocks of complex networks,” *Science*, vol. 298, no. 5594, pp. 824–827, 2002.
- [8] K. Newaz and T. Milenković, “Graphlets in network science and computational biology,” in *Analyzing Network Data in Biology and Medicine: An Interdisciplinary Textbook for Biological, Medical and Computational Scientists*, N. Pržulj, Ed. Cambridge University Press, 2019, ch. 5, p. 193–240.
- [9] M. Newman, A.-L. Barabási, and D. J. Watts, *The Structure and Dynamics of Networks*. Princeton: Princeton University Press, 2011.
- [10] G. Palla, I. Derényi, I. Farkas, and T. Vicsek, “Uncovering the overlapping community structure of complex networks in nature and society,” *Nature*, vol. 435, pp. 814–818, 2005.
- [11] M. Pósfai, Y.-Y. Liu, J.-J. Slotine, and A.-L. Barabási, “Effect of correlations on network controllability,” *Scientific Reports*, vol. 3, no. 1, p. 1067, 2013.
- [12] N. Pržulj, D. G. Corneil, and I. Jurisica, “Modeling interactome: Scale-free or geometric?” *Bioinformatics*, vol. 20, no. 18, pp. 3508–3515, 2004.
- [13] ———, “Efficient estimation of graphlet frequency distributions in protein-protein interaction networks,” *Bioinformatics*, vol. 22, no. 8, pp. 974–980, 2006.
- [14] X. Ren and J. Malik, “Learning a classification model for segmentation,” in *Proceedings Ninth IEEE International Conference on Computer Vision*, 2003, pp. 10–17 vol.1.
- [15] O. Rioul and M. Vetterli, “Wavelets and signal processing,” *IEEE Signal Processing Magazine*, vol. 8, no. 4, pp. 14–38, 1991.
- [16] A. Sarajlić, N. Malod-Dognin, Ö. N. Yaveroğlu, and N. Pržulj, “Graphlet-based characterization of directed networks,” *Scientific Reports*, vol. 6, no. 1, p. 35098, 2016.
- [17] C. E. Shannon, “A mathematical theory of communication,” *The Bell System Technical Journal*, vol. 27, pp. 379–423, 623–656, 1948.
- [18] ———, “Prediction and entropy of printed English,” *Bell System Technical Journal*, vol. 30, pp. 50–64, 1951.
- [19] N. Shervashidze, S. V. N. Vishwanathan, T. H. Petri, K. Mehlhorn, and K. M. Borgwardt, “Efficient graphlet kernels for large graph comparison,” in *Proceedings of the 12th International Conference on Artificial Intelligence and Statistics*, 2009, p. 8.
- [20] M. P. H. Stumpf, C. Wiuf, and R. M. May, “Subnets of scale-free networks are not scale-free: Sampling properties of networks,” *Proceedings of the National Academy of Sciences*, vol. 102, no. 12, pp. 4221–4224, 2005.
- [21] Ö. N. Yaveroğlu, N. Malod-Dognin, D. Davis, Z. Levnajic, V. Janjic, R. Karapandza, A. Stojmirovic, and N. Pržulj, “Revealing the hidden language of complex networks,” *Scientific Reports*, vol. 4, no. 1, p. 4547, 2015.
- [22] L. Ye and E. Keogh, “Time series shapelets: A new primitive for data mining,” in *Proceedings of the 15th ACM SIGKDD International Conference on Knowledge Discovery and Data Mining*, 2009, p. 947.